Check for updates

# Tectono-stratigraphy of the Eocene Zhu-1 Sub-basin in the Pearl River Mouth basin, China: controls on hydrocarbon source rock variability and implications

Pei Liu[1,2]*, Guangrong Peng[1,2], Ming Luo[1,2], Yuchen Wang[1,2], Wanlin Xiong[1,2], Penglin Song[1,2] and Guanyun Wu[1,2]

[1]Shenzhen Branch of CNOOC, Shenzhen, Guangdong, China, [2]Deepwater Development Ltd., CNOOC, Shenzhen, Guangdong, China

In rift basins, the vertical development and distribution of hydrocarbon source rocks show a makeable variability tightly linking to the tectono-stratigraphic interaction and evolution. This is also highly focused for petroleum industry, which is posing challenges for systematic hydrocarbon accumulation patterns. In the Zhu-1 Sub-basin of the Pearl River Mouth basin, the Eocene rift-related strata are important intervals for potential hydrocarbon exploration. This study analyzes the temporal and spatial attributes caused by tectonic transitions using 3D-seismic, drilling and logging well, and geochemical data, uncovering the impact of tectonic transition on the formation and development of hydrocarbon source rocks in the Eocene rift-related strata in the Zhu-1 Sub-basin. The results indicate that tectonic transitions caused by the HZ movement (~43 Ma) have affected the migration of the centers of depocenter and subsidence and drove the formation of two main hydrocarbon source rocks in the upper and lower sections of the Wenchang Formation. The migration of rifting activity has influenced the lateral distribution of high-abundance dark high-quality hydrocarbon source rocks, and expand the range of high-quality hydrocarbon source rocks. The half-graden styles in the different sag change associated with tectonic transitions, and basement uplift and magmatic bottoming reshape the internal stratigraphic structure of the half-graden, leading to the variability of hydrocarbon accumulations. The proposed three hydrocarbon distribution modes, gentle slope dominant, steep-slope dominant and double-slope dominant, were developed in different sags. These models provide important geological theoretical support for the search of potential large-scale hydrocarbon reservoirs in the Pearl River Mouth basin, South China Sea.

# 1 Introduction

Rift transition refers to the movement and geological effects of the crust within a specific region and stage of tectonic development, involving a regular displacement in a particular direction (Corti, 2009). This phenomenon is sometimes known as rift transitions or tectonic migration (Shi et al., 2009; Shi et al., 2017; 2020; Chen, 2003; Reemst and Cloetingh, 2000). It represents an important indicator of distinctive rift phases and the dynamic changes in the basin's geological setting (Xie et al., 1996; Corti, 2009; Reemst and Cloetingh, 2000; Ge et al., 2023; Ye et al., 2017; Wu et al., 2014; Henstra et al., 2017). Different tectonic settings exhibit distinct transitional characteristics, such as notable variations in rifting structure, fault geometry, and kinematics, as well as sedimentary and subsidence centers and kinetic mechanisms (Chen, 2003; Corti, 2009; Reemst and Cloetingh, 2000; Ye et al., 2017). These changes have extensive implications for hydrocarbon rocks, reservoir seals, traps, and the formation and distribution of oil and gas in sedimentary basins (Wu et al., 2014; Xia et al., 2007; Zhang et al., 2016; Liu et al., 2018).

The Zhu-1 Sub-basin in the Pearl River Mouth basin (PRMB) underwent complex tectonic movements during the Cenozoic era. It is composed of the Zhuqiong and Nanhai movements in the rift stage, as well as the Baiyun and Dongsha movements during the post-rift stage (Shi et al., 2009; Shi et al., 2017; Shi et al., 2020; Hao et al., 2021). In recent years, it has been discovered that there was a significant tectonic transitions in the Zhu-1 Sub-basin during the Eocene (Wang et al., 2024). The significant transition took place before and after 43 Ma (Shi et al., 2020). This transition mainly involved the north-south conversion of the rifting action, migration along the fault striking, basal uplift, magma movement, and stratigraphic erosion. This period is also namely as the HZ movement (Shi et al., 2009; Shi et at., 2017).

This paper systematically investigates the control mechanisms of rift transition on the formation and development of source rocks in the Zhu-1 Sub-basin from a tectono-stratigraphic perspective. Rift migration causes regular shifts in sedimentary centers, forming cyclical stratigraphic stacking patterns, with lacustrine mudstone segments developed during rift transition periods having the best hydrocarbon-generating potential. By integrating seismic techniques with geochemical data, this study aims to enhance our understanding of how tectonic activities influence the formation and preservation of hydrocarbon source rocks. Furthermore, deepening the study of the spatiotemporal coupling relationship between tectonostratigraphic evolution and source rock development can provide new geological evidence for the evaluation of hydrocarbon resource potential.

# 2 Geological background

The PRMB is a Cenozoic rifting basin located in the northern part of the South China Sea, with an area of about 17, 500 km$^2$ (Shi et al., 2008; Wang et al., 2024). It is situated at the intersection of the Indian plate, Pacific plate, and Eurasian plate (Shi et al., 2008; Ge et al., 2017; Wang et al., 2024). It consists of five major tectonic units, which from north to south are the northern fault zone, the northern depression zone (Zhu-1 and Zhu-3 Sub-basins), the

central uplift zone, the southern depression zone (Zhu-2 Sub-basin), and the southern uplift zone (Figure 1; Shi et al., 2009; Shi et al., 2017; Shi et al., 2020; Chen, 2003). The evolution of the PRMB mainly includes three stages, which are the Eocene-early Oligocene rift, the late Oligocene rift transition, and the early Miocene to Quaternary post-rift stages. Seven significant movements are observed, including the Zhuqiong-1, Huizhou, Zhuqiong-2, Nanhai, the Baiyun, and the Dongsha movement (Chen, 2003; Zhu et al., 2009; Zhong et al., 2014; Shi et al., 2009; Shi et al., 2017; Shi et al., 2020). During the rifting period, the Zhuqiong movements played a significant role in the tectonic transition (Chen, 2003; Shi et al., 2009; Shi et at., 2017; Shi et al., 2020).

The area of this study, the Zhu-1 Sub-basin, is situated in the northern part of the PRMB. It extends in the NE direction and runs roughly parallel to the coastline (Chen, 2003; Zhu et al., 2009; Shi et al., 2009). It is bordered by the northern uplift zone in the northwest, controlled by the Dongsha Uplift and the Panyu Low Uplift in the southeast. Additionally, it is bordered by the Zhu-3 Sub-basin to the southwest. The area can be further divided into several secondary tectonic units such as the Enping, Xijiang, Huizhou, and Lufeng Sag, arranged from west to east (Figure 1; Shi et al., 2009; Shi et al., 2017; Shi et al., 2020; Chen, 2003).

The stratigraphy in the PRMB includes the Wenchang, Enping, Zhuhai, Zhujiang, Hanjiang, Yuehai, and Wanshan Formation from bottom to top (Figure 2; Shi et al., 2009; Shi et al., 2017; Shi et al., 2020; Chen, 2003). Two distinct rift phases, namely rift phase 1 (RP1; early Eocene) and rift 2 (RP2; Late Eocene). Furthermore, the RP1 in the Zhu-1 Sub-basin can be divided into two sub-episodic stages, namely episodic RP1a (49–43 Ma) and RP1b (43–39 Ma), respectively (Figure 2; Chen, 2003; Shi et al., 2009; Shi et al., 2017; Shi et al., 2020). The basin is generally deepened in RP1a in response to the increase of fault activity intensity, while the lake expanded and been shallow as the decrease of fault activity.

Our target strata are the Wenchang and Enping Formation, specifically, the Wenchang Formation is further divided into two section, the lower Wenchang (WCSQ1, WCSQ2, WCSQ3) and upper Wenchang Formation (WCSQ4, WCSQ5, WCSQ6) from bottom to the top. Enping Formation is composed of four third-order sequences (EPSQ1, EPSQ2, EPSQ3, EPSQ4) (Shi et al., 2009; Shi et al., 2017). The Wenchang Formation features fan delta systems controlled by steep slope zones and small-scale braided river delta systems controlled by gentle slope zones (Zhao, 2016; Liu et al., 2019; Guo et al., 2022; Pang et al., 2022).

# 3 Data and methodology

## 3.1 Seismic data

This study employed pre-stack time-domain 3D seismic data and geochemical analysis to explore the intricate relationship between tectonic transitions and the distribution of hydrocarbon source rocks. The 3D seismic data utilized in this study spans a vast area of 19, 250 km$^2$, providing a comprehensive view of the subsurface geological structures. For the Wenchang Formation, the dominant seismic frequency ranges from approximately 20–30 Hz, which is crucial for identifying and characterizing geological features at different depths. This frequency range corresponds to a
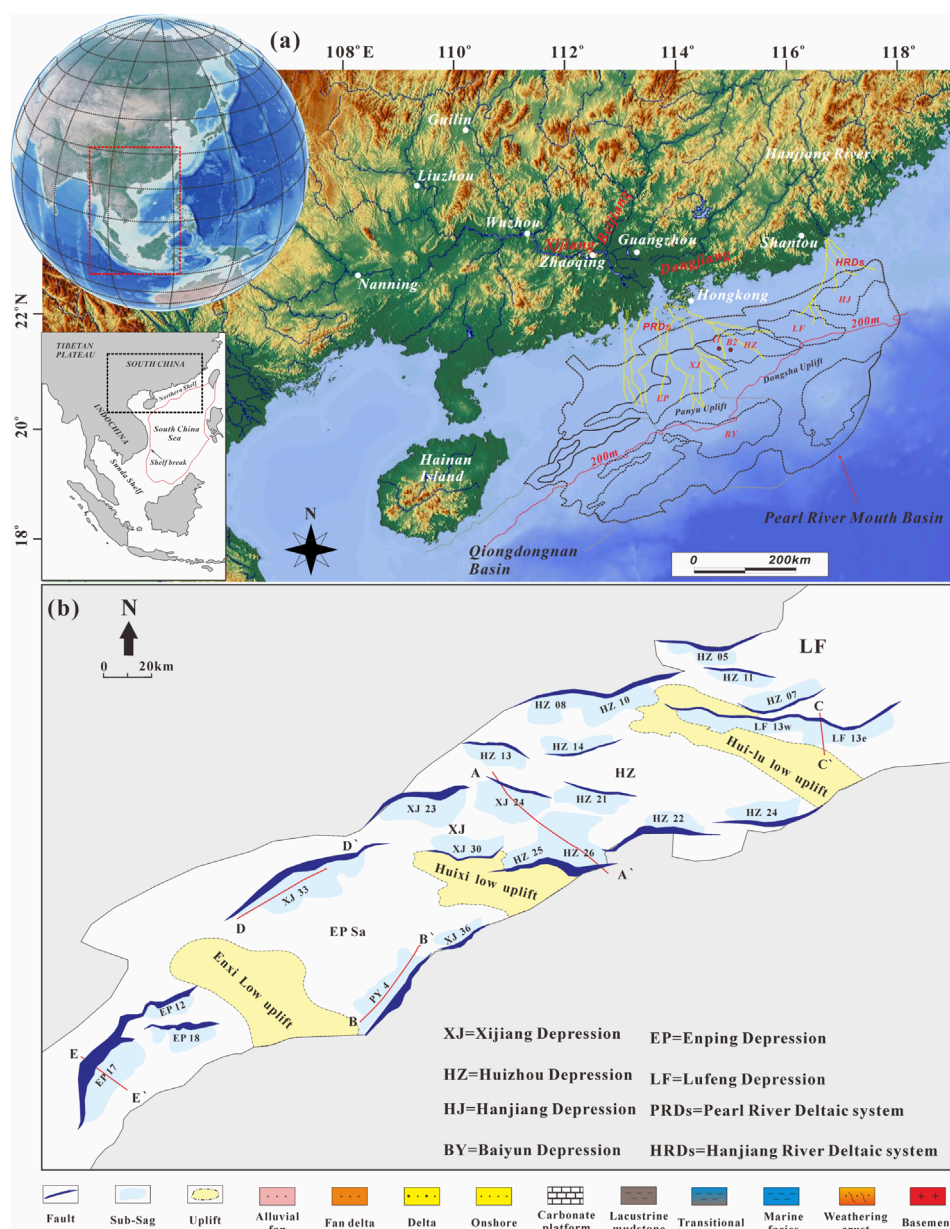
FIGURE 1
The geological location **(a)** and structural units **(b)** of the Zhu-1 Sub-basin, Pearl River Mouth Basin, China (summarized from Zhuo et al., 2015; Lin et al., 2018; Ge et al., 2017; Ge et al., 2023). Note that a total of 23 sags are developed in the Zhu-1 Sub-basin (including Enping, Xijing, Huizhou and Lufeng Depressions), seismic profiles AA' to EE' **(b)** are presented in Figures 5, 7.

vertical resolution of about 40–50 m, enabling detailed imaging of the stratigraphic layers and potential hydrocarbon reservoirs.

In the Zhu-1 Sub-basin, seismic profiles play a crucial role in identifying the fault combination fashions and sequence stratigraphic patterns (Guo et al., 2024; Yin et al., 2024). By interpreting the seismic data, we can delineate the boundaries of different geological structures (Guo et al., 2024; Yin et al., 2024). Based on these seismic interpretation boundaries, the fault displacement across various seismic boundaries is meticulously counted. This detailed analysis reveals the activity rules of faults, providing valuable insights into the tectonic evolution of the region.

## 3.2 Geochemistry data

Geochemical data samples from the LF13, PY4, and HZ26 Sags cover a range of key parameters that are of significant importance to geological research, more than 400 geographies in total. Specifically, the samples include Total Organic Carbon (TOC), an indicator that reflects the content of organic matter in rocks. Additionally, the total hydrocarbon potential (S1+S2) of the current rock samples was measured (Behar et al., 2001; Fu et al., 1991; Peters et al., 2005). This parameter integrates S1 and S2 and is used to assess the hydrocarbon generation potential of rocks. Moreover, the Hydrogen Index (HI)
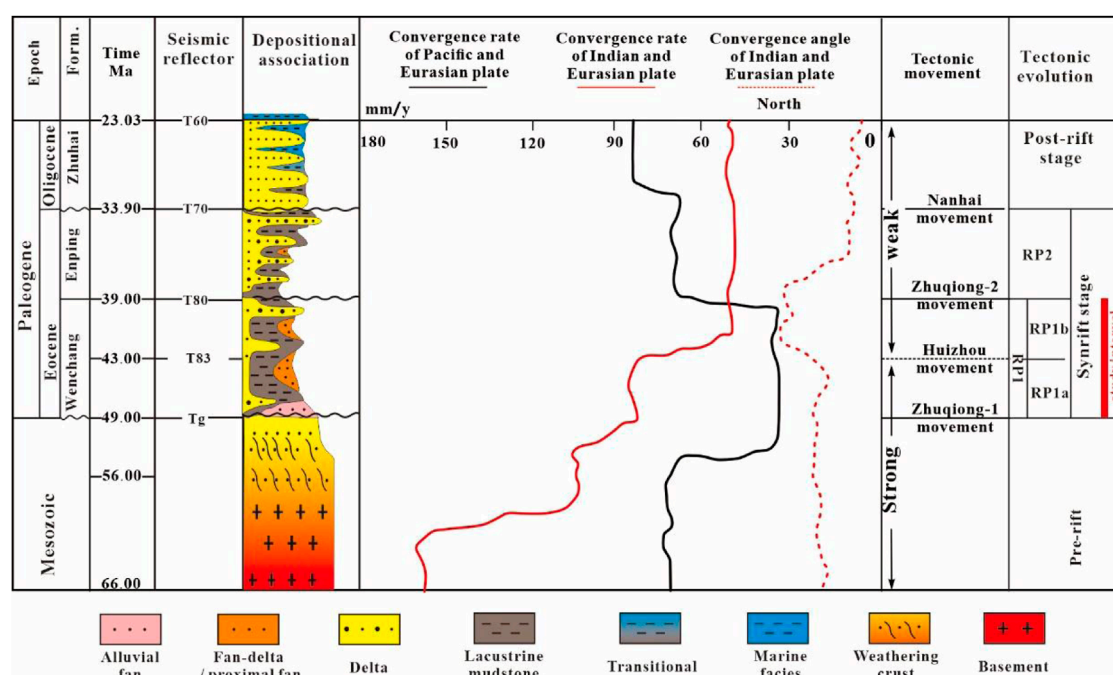
**FIGURE 2**
Eocene-Oligocene tectono-stratigraphic framework of the Zhu-1 Sub-basin, Pearl River Mouth Basin, China. Note that Zhuqiong-1 and Zhuqiong-2 movements are occurred at 49 Ma and 39 Ma, respectively. The Huizhou (HZ) movement was demonstrated to take place at 43 Ma, correlative to the transition of the distinctive plate activity (Ma et al., 2018; Shi et al., 2020; Ge et al., 2017; Hao et al., 2021; Ge et al., 2023). RP1 = Rift Phase 1 (49−39 Ma); RP2 = Rift Phase 2 (39−33.9 Ma); PR1a and PR1b is correlative to the early (49−43 Ma) and late (43−39 Ma) periods of PR1. Form. = Formation.

was recorded in the samples, which can be used to measure the type and maturity of organic matter (Fu et al., 1991; Peters et al., 2005). The temperature (Tmax) reflects the highest temperature reached by the rocks during pyrolysis and is closely related to the thermal maturity of organic matter (Cao et al., 2017; Ding et al., 2019). The vitrinite reflectance (Ro), an important indicator for assessing the maturity of organic matter, is also reflected in the sample data (Behar et al., 2001). Finally, the properties of kerogen were investigated in the samples. As the main organic component in rocks, the characteristics of kerogen play a key role in understanding geological history and the hydrocarbon generation process.

In addition to structural analysis, geochemical data are also essential for evaluating the hydrocarbon potential of the area. The quantity of free hydrocarbons is represented by the S1 peak, while the generative hydrocarbon potential is indicated by the S2 peak. The Tmax value corresponds to the pyrolysis temperature at which the maximum S2 yield is achieved (Cao et al., 2017; Ding et al., 2019). The sum of S1 and S2 values provides a comprehensive measure of the total hydrocarbon potential of the present rock samples. These geochemical parameters are critical in estimating the quality of the hydrocarbon source rocks, thereby aiding in the assessment of the hydrocarbon exploration potential.

## 3.3 The analysis of the fault activity

In our study, we selected 21 seismic profiles to investigate the fault activity. The displacement of the hanging wall and footwall of the fault was carefully measured and analyzed, as these displacements are key indicators of the fault activity. By examining the differences in displacement between the hanging wall and footwall, we can infer the nature and extent of the fault movement. This method allows us to quantify the fault activity and better understand the tectonic processes in these regions.

# 4 Results

## 4.1 Tectono-stratigraphy of Eocene Zhu-1 sub-basin

### 4.1.1 The characteristics and patterns of tectonic activity

The HZ Movement (~43 Ma) is associated with a series of tectonic activities, such as the north-southward shift of the rift center, displacement migration along the major fault, basement uplift, magmatic activity, and stratigraphic denudation (Shi et al., 2020).

In 49–39 Ma, the main tectonic changes occurred in the Huizhou, Lufeng, and Xijiang Sags (Figure 3). Notably, the most significant transformations took place in the southwestern part of the Huizhou Sag and the transition zone of the Huizhou-lufeng Low Uplift. The tectonic activities during this period were primarily focused on the basement uplifts of the Huixi Low Uplift and Huilu Low Uplift (Figure 4). This tectonic transition mainly led to the basement uplift of the western low uplift of the Huizhou Sag and

FIGURE 3
The calculated displacement (km) along the boundary faults in the selected sub-sags in the Zhu-1 Sub-basin of the Pearl River Mouth Basin. Note that the north-south transition and east-west migration along the orientation of the boundary faults. RP1a = Lower part of Wenchang Formation (49−43 Ma); RP1b = Upper part of Wenchang Formation (43−39 Ma).
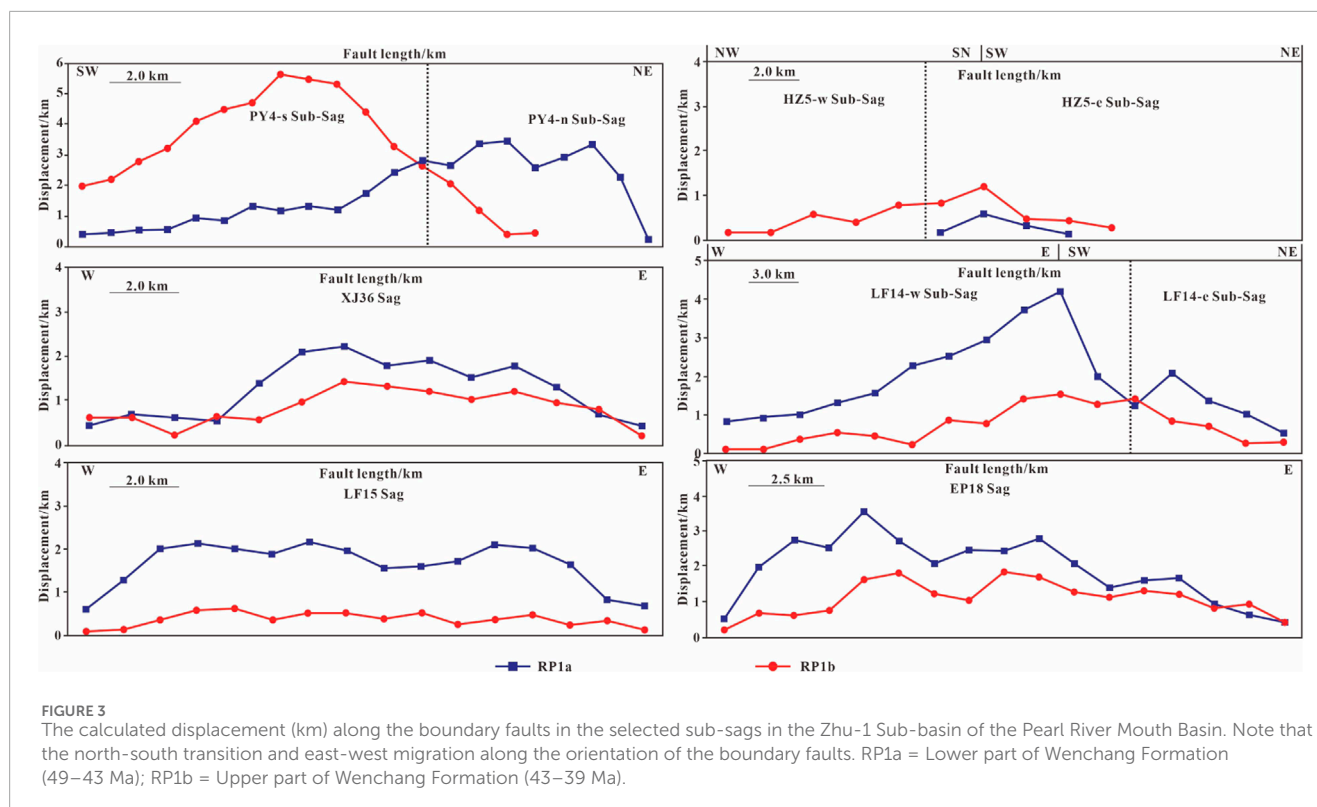
the Huizhou-Lufeng Low Uplift, as well as widespread stratigraphic denudation. Local magmatic intrusions reshaped the stratigraphic structure (Figures 4, 5), accompanying the northward shift of rifting and the migration of faults along the strike.

The north-south migration of tectonic activity showed the following three aspects (Figures 4, 5a): 1) the intensity of fault activity was strong in the south but weak in the north during 49–43 Ma, while it changed to be strong in the north but weak in the south during 43–39 Ma; 2) the combination pattern of faults shifted from a half-graben with a steep southern slope and a gentle northern slope, to another type of basin geometry correlating to a half-graben with a gentle southern slope associated a steep northern slope (Figure 5); 3) both the location of the subsidence center and the sedimentation rate of the sag center are characterized by a shift from south to north, such as the migration of fault centers from the southwest to the northeast (Figure 4).

### 4.1.2 The distribution patterns of depocentres

The migration of fault activity along the strike mainly shows the differential activity of controlling sag fault segmentation, which controls the orderly change of sedimentary center along the strike (Shi et al., 2020). For example, in the Xijiang Sag, the strata migrated regularly from east to west from the RP1a to the RP1b (Figures 4, 5b).

During 49–43 Ma, the sedimentary and thickness centers were relatively evenly distributed in the Zhu-1 Sub-basin, with the maximum thickness reaching up to 3,400 m (Figure 4a). During 43–39 Ma, the sedimentary and thickness centers were located in the northwest direction of the Zhu-1 Sub-basin, with the maximum thickness reaching up to 2,200 m (Figure 4b). Overall, the sedimentary and thickness centers migrated towards the

northwest of the basin. The patterns of depocenter distribution are similar to Shi et al. (2020).

## 4.2 Hydrocarbon rock distribution

### 4.2.1 Lateral migration of hydrocarbon rocks

During the Eocene, tectonic transitions triggered the migration of subsidence and depositional centers, which in turn influenced the movement of third-order sequences. The development of hydrocarbon source rock types and quality within these sequences exhibited significant spatial variability, driven by factors such as rift intensity, climate, and sedimentary filling (Zhu et al., 2016; Wang et al., 2015). The deep-lake facies correlative to source rocks are represented by of paralleled and medium- or high-amplitude seismic reflections, as evidenced by previous observations (Wu et al., 2014; Zhao, 2016; Zhu et al., 2016; Ge et al., 2023).

The migration of north-southward rifting locations show that the southern sub-sag belt had strong fault activity during 49–43 Ma, with subsidence and sedimentation centered in the south. In WCSQ3, fault activity peaked and formed a major hydrocarbon generation center (Figures 3, 4). In contrast, the northern sub-sags exhibited stronger fault activity, driving subsidence and deposition northward. This trend continued with a decreased fault activity in the early WCSQ4 stage and shifting the hydrocarbon generation center northward (Figures 3, 4).

From an east-west perspective, the eastern section showed an intense fault activity during 49–43 Ma, controlling subsidence and deposition on the east side. Fault activity peaked by WCSQ3, establishing a robust hydrocarbon generation center.

**FIGURE 4**
The tectonic transitions and the distribution of hydrocarbon source rock centres of the Wenchang Formation in the Zhu-1 Sub-basin, PRMB, China. **(a)** Lower part of Wenchang Formation (49−43 Ma); **(b)** Upper part of Wenchang Formation (43−39 Ma).

During 43–39 Ma, increased fault activity in the western section drove subsidence and deposition westward, with a waned activity and thus, the hydrocarbon generation center shifted westward (Figures 3, 4).

In conclusion, these north-south and east-west migrations of the hydrocarbon generation center governed the development of two distinct sets of high-quality, deep-lake facies source rocks with high organic abundance: one in the Lower part of the Wenchang Formation and the other in the Upper part of the Wenchang Formation.

## 4.2.2 Vertical development of hydrocarbon source rock

According to the geochemical characteristics of the hydrocarbon-rich sags, the two sets of main source rocks of the Wenchang Formation are high-quality dark mudstones with high organic matter abundance, large hydrocarbon generation potential and good kerogen type (Shi et al., 2020).

The organic matter abundance of WCSQ3 of the PY4 Sag is up to 11.23%, the maximum hydrocarbon generation potential is 87.35 mg/g, the maximum hydrogen index is 746 mg hydrocarbon/g TOC, and the kerogen type is $II_1$-I type (Table 1; Figure 6). The

organic matter abundance in the WCSQ4 reaches up to 10.54%, the maximum hydrocarbon potential is 76.08 mg/g, and the maximum hydrogen index is 808 mg hydrocarbon/g TOC, and the type of kerogen is $II_1$-I (Table 1; Figure 6).

The organic matter abundance of WCSQ3 of the LF13 Sag reaches up to 7.75%, the maximum hydrocarbon potential is 28.82 mg/g, the maximum hydrogen index is 606 mg hydrocarbon/g TOC, and the type of kerogen is $II_1$-$II_2$ (Table 1; Figure 6). The organic matter abundance in the Upper Wenchang Formation reaches up to 5.12%, the maximum hydrocarbon potential is 23.23 mg/g, and the type of kerogen is $II_1$-$II_2$ (Table 1; Figure 6).

The hydrocarbon source rocks of the Lower Wenchang Formation are also observed in the HZ26 Sag. The organic matter abundance of the WCSQ3 is up to 8.14%, the maximum hydrocarbon potential is 44.22 mg/g, the maximum hydrogen index is 602 mg hydrocarbon/g TOC, and a kerogen type is $II_1$ (Table 1; Figure 6). In addition to the main hydrocarbon source rock intervals, hydrocarbon source rocks are also distributed in several other third-order sequences of the Wenchang Formation, but their organic matter content is obviously reduced and their quality deteriorates. Obviously, the tectonic transition has changed the distribution of high-abundance dark mudstone succession and
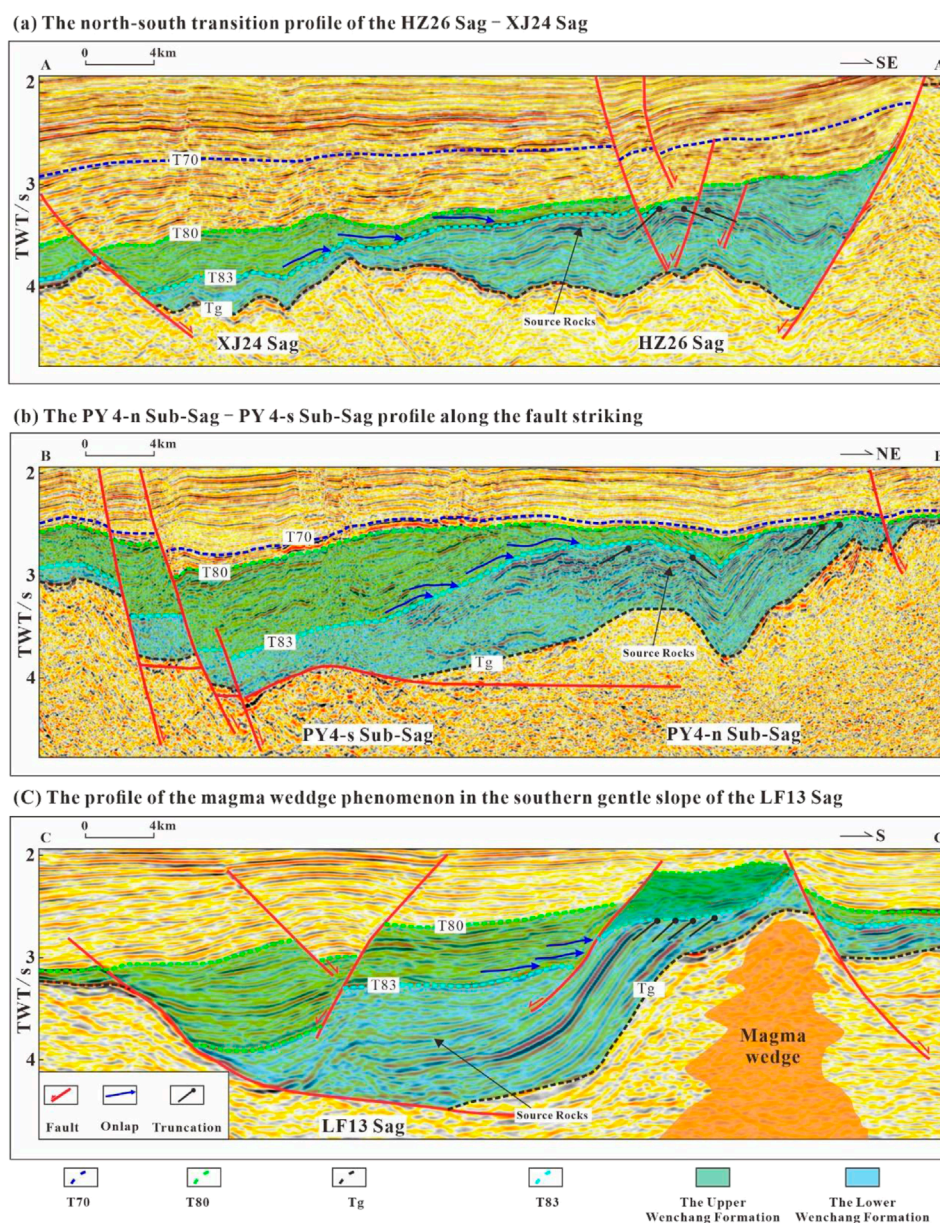
**FIGURE 5**
The stratigraphic typical geological phenomena of the tectonic transition during the Wenchang Formation in the Zhu-1 Sub-basin of the PRBM (see Figure 1 for the locations of the seismic profiles). The PY4-n and PY4-s Sub-sag is the north and south of the PY4 Sag, respectively. **(a)** The north-south transition profile of the HZ26 Sag - XJ24 Sag, **(b)** The PY 4-n Sub-Sag - PY 4-s Sub-Sag profile along the fault striking, **(c)** The profile of the magma weddge phenomenon in the southern gentle slope of the LF13 Sag.

controlled the vertical development of high-quality hydrocarbon source rocks.

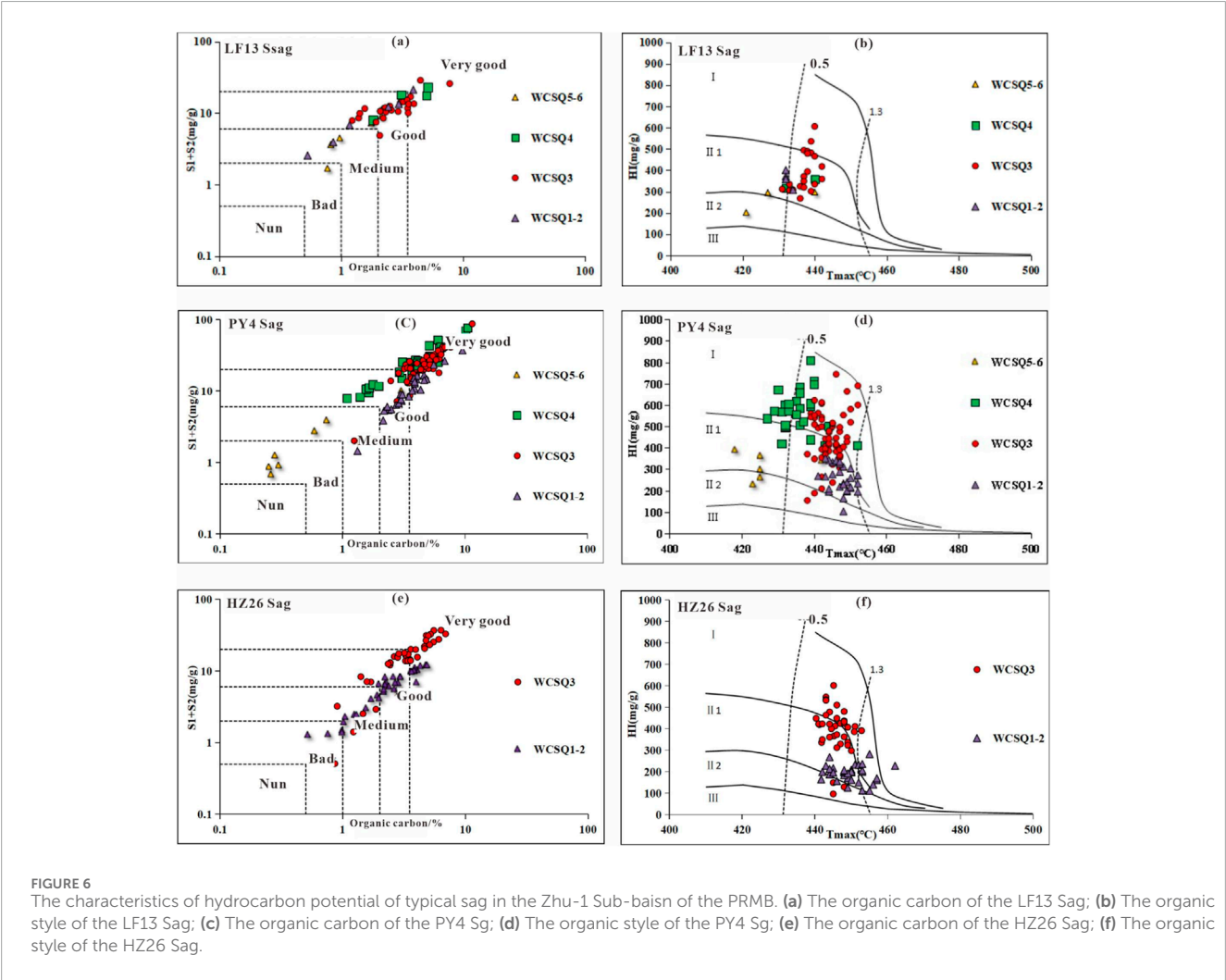### 4.2.3 Distribution of hydrocarbon-rich depressions

The hydrocarbon source rock fundamentally affects the distribution and enrichment of hydrocarbons (Hu and Huang, 1991). The transition and migration of the main hydrocarbon source rocks make the oil and gas supply no longer limited to a local area in the hydrocarbon-bearing basins, and form a wide range of hydrocarbon centers on the planar surface (Figure 4) which greatly widens the range of hydrocarbon-rich depressions and promotes the accumulation of the oil and gas in groups.

During the transition of hydrocarbon source rocks across faults, the main hydrocarbon source rocks of the lower part of the Wenchang Formation were developed during 49–43 Ma (Figure 5; WCSQ3). The hydrocarbon source rocks distributed mainly in the southeastern part of the depressions, which was promoting the formation of hydrocarbon-rich sub-sag, such as the LF15, LF13 and HZ26 Sags, and so on (Figure 4). The main hydrocarbon source rocks of the Upper part of the Wenchang Formation were developed WCSQ4. It was mainly distributed in the northwestern part of the

**TABLE 1** The geochemical characteristics of hydrocarbon source rocks in the Wenchang Formation in the Zhu-1 Sub-basin of the Pearl River Mouth basin. WC Form. = Wenchang Formation.

| | Sag | Strata | Depth (m) | TOC (%) | S1+S2 (mg/g) | HI (mg/g) | Tmax (°C) | Ro (%) | Kerogen type | Source rock quality |
|---|---|---|---|---|---|---|---|---|---|---|
| PY 4 | Upper WC Form. | WCSQ5-6 | 3562 | 2.79 | 9.73 | 341.9 | 442 | / | II | Medium |
| | | WCSQ4 | 3273~3747.5 | 0.5~10.54 | 1.13~76.08 | 136.3~711.6 | 427~452 | 0.63~0.66 | $II_1$ | Good |
| | Lower WC Form. | WCSQ3 | 3422~3919.6 | 0.76~11.43 | 0.09~87.35 | 156.5~745.8 | 433~449 | 0.60~0.95 | $II_1$ | Good |
| | | WCSQ1-2 | 4000~4120 | 2.18~4.84 | 5.31~16.67 | 196.8~342.9 | 441~452 | 0.94~1.08 | II | Medium |
| LF 13 | Upper WC Form. | WCSQ5-6 | 3438~4092 | 0.97~2.13 | 3.64~9.14 | 260~377 | 402~459 | 0.55~0.70 | $II_2$ | Medium-Good |
| | | WCSQ4 | 3594~3624 | 1.82~5.12 | 8.09~23.24 | 283~359 | 420~440 | 0.56~0.57 | $II_2$ | Good |
| | Lower WC Form. | WCSQ3 | 3651~3882 | 1.75~3.70 | 2.96~11.61 | 306~569 | 431~471 | 0.59~0.77 | $I$-$II_2$ | Good |
| | | WCSQ1-2 | 3915~4062 | 0.84~2.43 | 0.29~12.30 | 361~402 | 425~471 | 0.74~0.88 | $II_1$-$II_2$ | Medium-Good |



**FIGURE 6**
The characteristics of hydrocarbon potential of typical sag in the Zhu-1 Sub-baisn of the PRMB. **(a)** The organic carbon of the LF13 Sag; **(b)** The organic style of the LF13 Sag; **(c)** The organic carbon of the PY4 Sg; **(d)** The organic style of the PY4 Sg; **(e)** The organic carbon of the HZ26 Sag; **(f)** The organic style of the HZ26 Sag.

sag, which makes the sag have the strong capacity of hydrocarbon-generation, such as the XJ24 and the HZ10 Sags (Figure 4).

During the migration of the hydrocarbon source rocks along the fault striking or dipping, the Upper and Lower parts of the Wenchang Formation show a lateral stacking pattern in the EP17 and the PY4 Sags. The two sets of main hydrocarbon sources of the WCSQ3 and WCSQ4 are laterally stacked and have a relatively largescale, which ensures a strong hydrocarbon (Figure 4). The main hydrocarbon source rocks of the Wenchang Formation in the Zhu-1 Sub-basin have been migrated along faults so that the hydrocarbon-rich depressions are distributed from south to north and from east to west, which has broadened the range of oil supply.

# 5 Discussions

## 5.1 Controls of rift transition on hydrocarbon rocks distribution variability

The northern margin of the South China Sea lies at the intersection of the Indian-Australian, Eurasian, and Pacific plates, influenced by the Tethys and Pacific tectonic domains (Northrup et al., 1995; Lee and Lawver, 1995; Guo et al., 2001; Suo et al., 2012). The PRMB reflects these regional tectonics (Figure 2). The Indian-Eurasian plate collision began around 43 Ma, reducing convergence rates and causing extrusion of the Indian-Chinese and South China landmasses. Concurrently, the Pacific Plate subduction direction shifted from NNW to NWW, coinciding with the HZ Movement (Shi et al., 2020). Detrital zircons in the Wenchang Formation of the Zhu-1 Sub-sag, with a peak age of 48–43 Ma, likely record magmatism during this period, aligning with the age inferred from lake basin sedimentation rates and regional tectonic events (Wang et al., 2017). The tectonic transition within the episode controlled the temporal and spatial evolution characteristics of the rifting activities, sedimentation centers, and sedimentary sequences (Zhu, 2007; Wang et al., 2017). This, in turn, affected the formation and development of hydrocarbon source rocks. These factors play an important role in controlling the distribution of high-quality hydrocarbon source rocks, the formation of hydrocarbon-rich depressions, and the gathering of hydrocarbon (Zhu, 2007; Wang et al., 2017).

Tectonic transitions led to the migration of sedimentary centers of different third-order sequences and the development of hydrocarbon source rocks in lateral stacking patterns (Figure 7), which is conducive to the formation of widely distributed hydrocarbon centers and greatly broadens the scope of hydrocarbon rich depressions (Shi et al., 2020). This motif is completely different from the development mode of hydrocarbon source rocks in the independent hydrocarbon centers of the inherited depressions, and the huge thickness of the sedimentary mudstones (Figure 5).

The tectonic transitions lead to obvious temporal and spatial migration characteristics of hydrocarbon source rocks (Zhu et al., 2016; Wang et al., 2015). The migration pattern of different sags shows a variability, including the three ways of north-south conversion across faults, migration along the fault strike, and self-migration along the fault tendency. The north-south transition is driven by rifting movements, particularly evident in the Huizhou and Lufeng Depressions. During RP1a (Figure 7), strong southern fault activity was localized subsidence and deposition in the south, with main hydrocarbon source rocks in the Lower part of the Wenchang Formation (e.g., HZ26, LF15, LF13 Sags). In RP1b, increased displacement of the northern fault after the rift transition (43 Ma) shifted the subsidence and deposition centers northward. The main hydrocarbon source rocks then shifted to the Upper part of the Wenchang Formation (e.g., XJ24, HZ10, LF7 Sags). This rifting transition caused the migration and dislocation of hydrocarbon source rocks from south to north (Figure 7a).

Heterogeneous migration in the Xijiang Depression is driven by sequence stratigraphic shifts along fault strikes (Figure 7). Influenced by tectonic transitions, the boundary faults are highly active, causing significant migration of depocenters along the fault strike from the early to the late of Eocene. As shown in Figure 7b, a "see-saw"-style thickness variation is observed from RP1a to RP1b. Early fault activity was stronger in the east, while late activity was stronger in the west. This differential fault activity led to the migration of depositional centers and hydrocarbon source rocks along the faults (Figure 7).

In contrast, self-migration in the EP Sag is characterized by the development of rift effects along the boundary fault striking direction. Controlled by tectonic transitions, the sedimentary centers migrate along the fault dip from the RP1a to RP1b, resulting in lateral superposition of hydrocarbon source rocks along the fault dip (Figure 7c).

Tectonic transitions lead to changes in the fault structure, changes in the styles of sequences stratigraphy, stratum uplift, and uptilting direction is often a low-potential area of hydrocarbons. Hydrocarbons are more likely to be transported to the direction of the stratigraphic warping, thus affecting the dominance of the accumulation of hydrocarbons (Zhu et al., 2015; Jiang et al., 2015; Jiang et al., 2019; Zhang et al., 2017; Liu et al., 2013; Shi, 2013).

## 5.2 Controls of rift transition on hydrocarbon accumulation pattern variability

### 5.2.1 Controls of the rifting transitions on stratigraphy dipping pattern

The half-graben structure is the basic unit of rift basin, including simple half-graben and complex half-graben, and other types (Rosendahl, 1986; Steckler, 1985; Ru, 1990; Martínez Candela et al., 2024; Tian et al., 2024).

Commonly, under the condition that sedimentary filling and extensional deformation are in equilibrium and the evolution mechanism of the boundary fault remains unchanged. The sequence on the steep slope side of the half-graben faults will be offlapping, forming a progradational sequence architecture, and the gentle slope away from the faults will be overlapping, which is correspondingly called the retrogradational sequence pattern (Naseer, 2025). This causes the basin to show "lateral accretion" on the macroscopic level, with the sequence overlapping the gentle slope step by step, and stripping at the edge (Qi et al., 1997). The tectonic evolution and sedimentary infilling pattern of the half-graben determined that the gentle slope is the dominant direction of the strata pinch out (Figure 7). Under this background, the hydrocarbon source rock strata are uplapping to the gentle slope, which makes the gentle
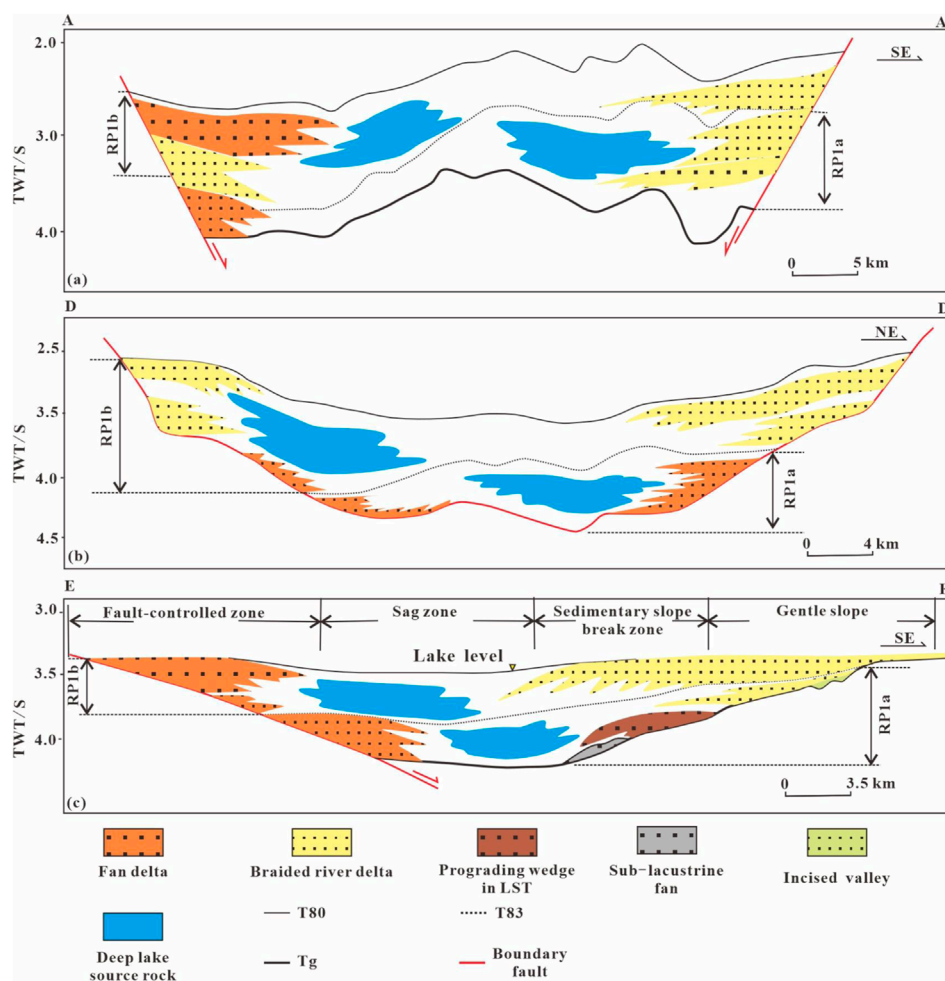
FIGURE 7
The migration pattern of hydrocarbon source rocks in the Wenchang Formation in the Zhu-1 Sub-basin of the PRMB. The locations of **(a–c)** profiles see Figure 1. **(a)** The Huizhou Depression: north-south transition model across the faults; **(b)** The Xijiang Depression: heteromigration model along the fault striking; **(c)** The Enping Depression: self-migration model along the fault dipping.
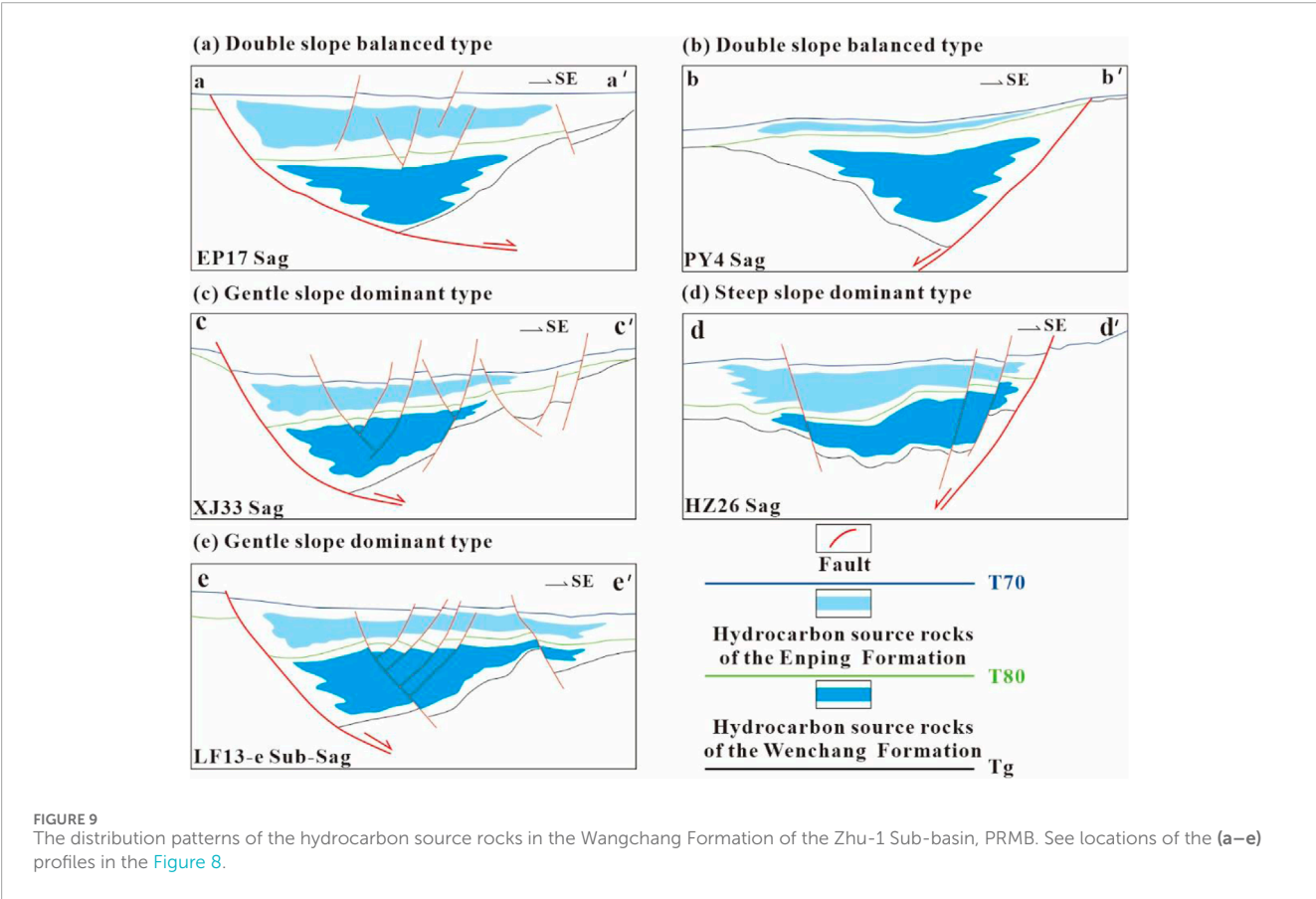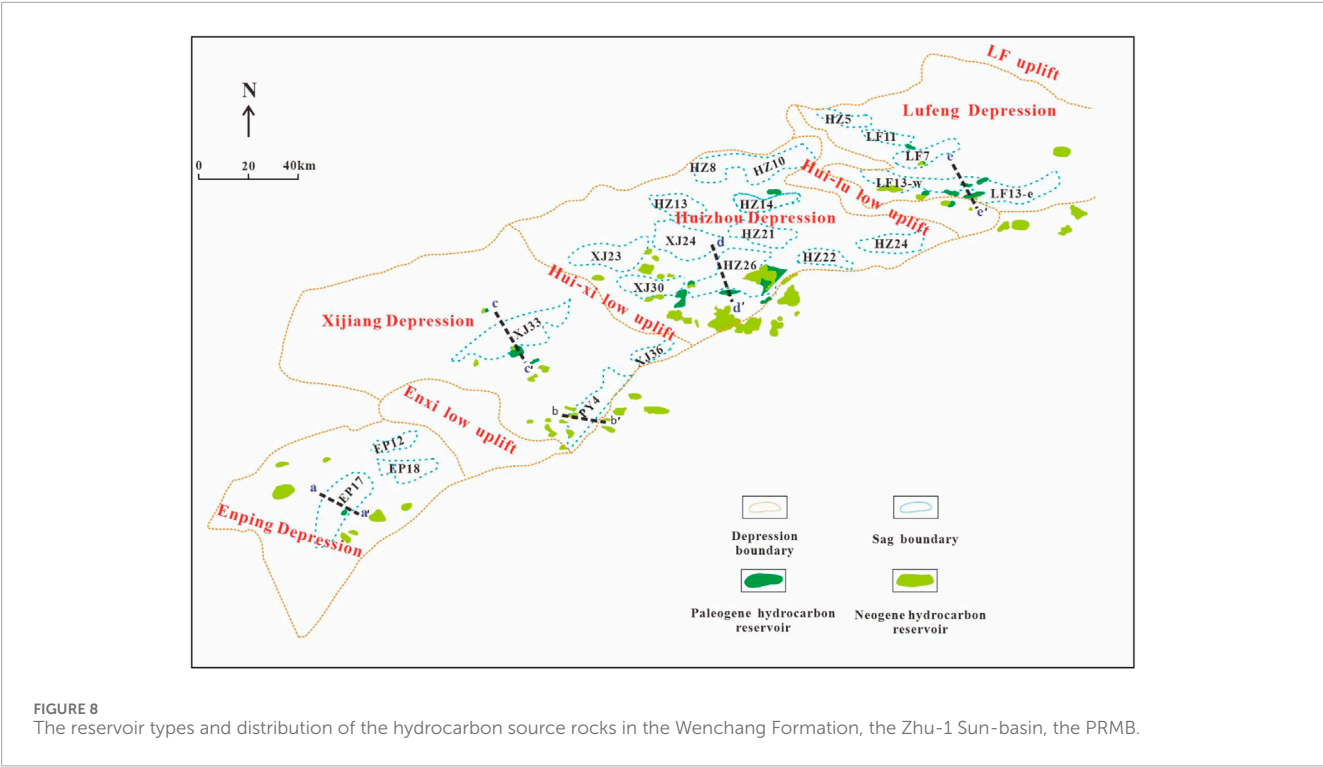
slope become the dominant direction of hydrocarbon drainage and convergence (Zhu et al., 2015; Jiang et al., 2015; Jiang et al., 2019; Qi et al., 1997; Liu et al., 2015; Allen and Allen, 2005).

During rifting basin formation, the half-graben structure evolves with varying tectonic influences, altering its internal sequence architecture (Allen and Allen, 2005; Naseer, 2025). In the Zhu-1 Sub-sag, tectonic transitions modified the half-graben structure and sedimentary patterns. The north-south rifting shift caused the half-graben style to transition from having a steep southern slope and gentle northern slope to the opposite configuration. For instance, the fault system in the Huizhou Depression and the up-dip contact of sedimentary sequences and hydrocarbon source rocks migrated northward after 43 Ma (Figure 4). The basement uplift and magmatic basement breakup caused the stratigraphy to be deformed at a later stage, which changed the stratigraphic occurrence (Allen and Allen, 2005; Schirripa et al., 2024). The gentle slope in the LF13 Sag was further rotationally uplifted by the effect of magma diapir, making stratigraphy sequence and hydrocarbon source rock warp towards the gentle slopes (Figure 5).

## 5.2.2 Controls of the rifting transitions on petroleum accumulation patterns

According to the evolution rule of the half-graben structure and hydrocarbon source rocks occurrence, three dominant convergence styles were summarized in the Zhu-1 Sub-basin, which are the gentle slope dominant, steep slope dominant, and double slope balanced types (Figures 8, 9).

The gentle slope type is mainly distributed in the LF13 and XJ33 Sags (Figure 9). The consistent active boundary faulting promoted the continuing subsidence around the steep slopes in the both northwestern and northwestern parts, and thus, the high-quality hydrocarbon source rocks overlapped and thinned to the gentle slope in LF13 Sag. In Eocene, the magmatic diapir made the bedrock block of the gentle slope uplift in a southwesterly direction and the hydrocarbon source rock further dip to the gentle slope (Mi et al., 2018). This area became the low-potential area of the oil and gas accumulations, and provided a good background for the accumulation of hydrocarbons to the southwest. The discovery of the oil and gas in this kind of depression is mainly concentrated in the direction of convergence of the gentle slope (Mi et al., 2018).

**FIGURE 8**
The reservoir types and distribution of the hydrocarbon source rocks in the Wenchang Formation, the Zhu-1 Sun-basin, the PRMB.



**FIGURE 9**
The distribution patterns of the hydrocarbon source rocks in the Wangchang Formation of the Zhu-1 Sub-basin, PRMB. See locations of the **(a–e)** profiles in the Figure 8.

The steep slope dominant type is primarily found in HZ26, XJ24, and XJ30 Sags (Figure 9). As shown in Figure 8, the persistent activity of the southwest fault during 49–43 Ma facilitated the development of dark mudstone in the HZ26 Sag. During 43–39 Ma, rapid uplift of the southwest area reversed the hydrocarbon source rock strata toward the steep slope, favoring southwestward hydrocarbon accumulation (Shi et al., 2020; Mi et al., 2018). Exploration confirms that in this direction, Paleogene and Neogene oil and gas reservoirs are distributed in clusters and belts.

The double slope balanced type is mainly developed in the PY4 and EP17 Sags. In the EP17 Sag, tectonic transitions caused migrations of sedimentary and subsidence centers along fault trends from RP1a to RP1b (Figures 4, 9). High-quality hydrocarbon source rocks migrated and superimposed along the fault dip, resulting in the lower part of the Wenchang Formation dipping gently southwest and the upper part of the Wenchang Formation dipping steeply northeast. These two sets of source rocks converge toward the flanks in different sags, with commercial oilfield clusters now formed in both the northern and southern sides (Figure 9).

## 5.3 Implications for hydrocarbon source rocks in rift basins

The distribution of source rocks in rift basins is influenced by both climate and tectono-sedimentary interactions, exhibiting a significant complexity (Zeng et al., 2025; Tajmir et al., 2021; Schirripa et al., 2024; Naseer, 2025). Differences in tectonic activity episodes lead to variations in basin subsidence rates and sedimentary environments, which in turn affect the development and distribution of source rocks (Zeng et al., 2025). For example, the intense rifting in the Beibu Gulf Basin during the early Eocene led to rapid subsidence of the lake basin, forming semi-deep lake to deep lake facies mudstone and shale, which provided favorable conditions for the development of high-quality source rocks (Zhou et al., 2024). Meanwhile, climatic conditions affect the provenance supply and sedimentation rates of sediments, further influencing the thickness and organic matter content of source rocks (Shi et al., 2024). This complex geological background makes the hydrocarbon accumulation process subject to multiple constraints, increasing the complexity of hydrocarbon accumulation (Tajmir et al., 2021; Schirripa et al., 2024).

To improve the accuracy of hydrocarbon exploration, rift basins must be subdivided into different tectonic activity episodes and structural zones for study (Zhou et al., 2024). The distribution patterns and hydrocarbon generation potential of source rocks vary under the different tectonic activity episodes (Naseer, 2025), while the division of structural zones helps clarify the pathways and accumulation sites of hydrocarbons (Chen et al., 2021). By conducting research based on different tectonic activity episodes and structural zones, it is possible to confidently predict favorable hydrocarbon accumulation zones, thereby providing a scientific basis for hydrocarbon exploration.

# 6 Conclusion

The tectonic shift within the rift phase in Zhu-1 Sub-basin is mainly manifested as rifting migration, basement uplift, and magmatic underplating, which affects the formation and development of hydrocarbon source rocks. The key conclusions are summarized as follows:

(1) The tectonic shift caused the hydrocarbon center to shift from north to south and migrate from east to west, forming two sets of main hydrocarbon source rocks in the upper and lower sections of the Wenchang Formation, changing the distribution of high-abundance dark mudstone layers, and controlling the vertical development of high-quality hydrocarbon source rocks.

(2) The tectonic transformation caused the main hydrocarbon source rocks to show obvious migration in space and time, with three motifs: north-south conversion across faults, heterogeneous migration along faults, and self-migration along faults, which made the high-quality hydrocarbon source rocks laterally stacked and greatly broadened the range of hydrocarbon-rich depressions.

(3) The structure of the half-graben changed with the tectonic transformation, and the basement uplift and magmatic underplating remodeled the internal stratigraphic structure of the half-graben, restricting the stratigraphy of the hydrocarbon source rocks and forming three hydrocarbon convergence modes of the gentle slope dominant, steep slope dominant, and double slope balanced types in different depressions and sags.

(4) The study reveals that the quality of source rocks in the Eocene Wenchang Formation of the Zhu-1 Sub-basin is significantly correlated with the intensity of syn-depositional faulting, with the structural flexure zone formed during the rift phase 1 (49–39 Ma) controlling the belt-like distribution of high-quality source rocks.

# Data availability statement

The original contributions presented in the study are included in the article/supplementary material, further inquiries can be directed to the corresponding author.

# Author contributions

PL: Writing – original draft, Writing – review and editing. GP: Writing – review and editing. ML: Writing – review and editing. YW: Writing – review and editing. WX: Writing – review and editing. PS: Writing – review and editing. GW: Writing – review and editing.

# Funding

supported by the CNOOC "14th Five-Year Plan" Major Science and Technology Project (Grant No. KJGG2022-0403) and the Shenzhen Branch of CNOOC Major Productive and Scientific Research Projects (SCKY-2024-SZ-YJYKT-01).

The authors declare that this study received funding from CNOOC. The funder had the following involvement in the study: data collection.

## Generative AI statement

The author(s) declare that no Generative AI was used in the creation of this manuscript.

## Conflict of interest

Authors PL, GP, ML, YW, WX, PS, and GW were employed by Shenzhen Branch of CNOOC. Authors PL, GP, ML, YW, WX, PS, and GW were employed by Deepwater Development Ltd., CNOOC.

## Publisher's note

All claims expressed in this article are solely those of the authors and do not necessarily represent those of their affiliated organizations, or those of the publisher, the editors and the reviewers. Any product that may be evaluated in this article, or claim that may be made by its manufacturer, is not guaranteed or endorsed by the publisher.

## References

Allen, P. A., and Allen, H. R. (2005). *Basin analysis:principles and applications*. Oxford: Blackwell Publishing Ltd.

Behar, F., Beaumont, V., and Penteado, H. D. B (2001). Rock-Eval 6 technology: performances and developments. *Oil Gas Sci. Technol.* 56 2, 111–134. doi:10.2516/ogst:2001013

Cao, Z., Liu, G., Xiang, B., Wang, P., Niu, G., Niu, Z., et al. (2017). Geochemical characteristics of crude oil from a tight oil reservoir in the Lucaogou Formation, Jimusar sag, Junggar Basin. *AAPG Bull.* 101, 39–72. doi:10.1306/05241614182

Chen, C. M. (2003). *The conditions for hydrocarbon accumulation in the eastern Pearl River Mouth Basin*. Beijing: Science Press.

Chen, H. H., Wood, L. J., and Gawthorpe, R. L. (2021). Sediment dispersal and redistributive processes in axial and transverse deep-time source-to-sink systems of marine rift basins: Dampier Sub-Basin, Northwest Shelf, Australia. *Basin Research* 33 (1), 227–249. doi:10.1111/bre.12462

Corti, G. (2009). Continental rift evolution: from rift initiation to incipient break-up in the Main Ethiopian Rift, East Africa. *Earth-Science Rev.* 96 (1/2), 1–53. doi:10.1016/j.earscirev.2009.06.005

Ding, X., Qu, J., Imin, A., Zha, M., Su, Y., Jiang, Z., et al. (2019). Organic matter origin and accumulation in tuffaceous shale of the lower Permian Lucaogou Formation. *Jimsar Sag. J. Pet. Sci. Eng.* 179, 696–706. doi:10.1016/j.petrol.2019.05.004

Fu, J., Sheng, G., Xu, J., Jia, R., Fan, S., Peng, P., et al. (1991). Application of biomarker compounds in assessment of paleoenvironments of chinese terrestrial sediments. *Geochimica* 1, 1–12. doi:10.1016/0146-6380(90)90116-H

Ge, J. W., Dong, Y. H., Tan, M. X., Chen, H. H., Sun, L. P., Li, S. L., et al. (2023). Teconostratigraphy of Paleogene zhu-3 depression of the Pearl River Mouth basin, south China sea: implications for syn-rift architecture in multiphase rifts. *Mar. Petroleum Geol.* 155, 106389. doi:10.1016/j.marpetgeo.2023.106389

Ge, J. W., Zhu, X. M., Zhang, X. T., Jones, B. G., Yu, F. S., Niu, Z. C., et al. (2017). Tectono-stratigraphic evolution and hydrocarbon exploration in the Eocene southern lufeng depression, Pearl River Mouth basin, south China sea. *Aust. J. Earth Sci.* 64 (7), 931–956. doi:10.1080/08120099.2017.1370613

Guo, L. Z., Zhong, Z. H., Wang, L. S., Shi, Y. S., Li, H., and Liu, Z. W. (2001). Regional tectonic evolution around yinggehai basin of south China sea. *Geol. J. China Univ.* 7 (1), 1–12. doi:10.1016/S1006-5494(01)60021-0

Guo, R., Shi, J. X., Jiang, S. Y., Jiang, S., and Cai, J. (2024). Prediction of structural fracture distribution and analysis of controlling factors in a passive continental margin basin. *Appl. Sci.* 14 (16), 7271. doi:10.3390/app14167271

Guo, W., Xu, G. Q., Chen, Z. M., Li, X., Xiang, X. H., and Liu, D. D. (2022). Sedimentary filling characteristics and evolution of the Paleogene Wenchang Formation in Bai yun main sag, Pearl River Mouth basin. *J. Palaeogeogr. (ChineseEdition)* 24 (1), 112–128. doi:10.7605/gdlxb.2022.01.009

Hao, S. H., Mei, L. F., Shi, H. S., Paton, D., Mortimer, E., Du, J. Y., et al. (2021). Rift migration and transition during multiphase rifting: insights from the proximal domain, northern South China Sea rifted margin. *Mar. Petroleum Geol.* 123, 104729–729. doi:10.1016/j.marpetgeo.2020.104729

Henstra, G. A., Gawthorpe, R. L., Helland-Hansen, W., Ravnås, R., and Rotevatn, A. (2017). Depositional systems in multiphase rifts: seismic case study from the Lofoten margin, Norway. *Basin Res.* 29 (4), 447–469. doi:10.1111/bre.12183

Hu, J. Y., and Huang, D. F. (1991). *The theoretical basis of Chinese terrestrial petroleum geology*. Beijing: Petroleum Industry Press.

Jiang, Y. L., Liu, H., Song, G. Q., Wang, Y. S., Liu, P., and Lu, X. Y. (2015). Relationship between geological structures and hydrocarbon enrichment of different depressions in the bohai bay basin. *Acta Geol. Sin. Engl. Ed.* 40 (5), 1998–2011. doi:10.1111/1755-6724.12613

Jiang, Y. L., Su, S. M., Liu, H., Wang, Y. S., and Liu, J. D. (2019). Types of Cenozoic sedimentary subsgs and their relationship with hydrocarbon enrichment in Bohai Bay Basin. *Acta Pet. Sin.* 40 (6), 635–645. doi:10.7623/syxb201906001

Lee, T., and Lawver, L. A. (1995). Cenozoic plate reconstruction of southeast asia. *Tectonophysics* 251, 85–138. doi:10.1016/0040-1951(95)00023-2

Lin, C. S., Jiang, J., Shi, H., Zhang, Z., Liu, J., Qin, C., et al. (2018). Sequence architecture and depositional evolution of the northern continental slope of the South China Sea: responses to tectonic processes and changes in sea level. *Basin Res.* 30, 568–595. doi:10.1111/bre.12238

Liu, B. B., Yu, X. H., Wu, J. F., Liao, Z. B., Du, Y. H., Gao, Z. P., et al. (2015). Research on half-garben types and sedimentary filling modes of northern continental margin basin of the South China Sea. *J. China Univ. Min. Technol.* 44 (33), 498–506. doi:10.13247/j.cnki.jcumt.000258

Liu, B. J., Pang, X., Wang, J. H., Ren, J. Y., Liu, J., Zheng, J. Y., et al. (2019). Sedimentary system response process and hydrocarbon exploration significance of crust thinning zone at extensional continental margin of deep-water area in Pearl River Mouth Basin. *Acta Pet. Sin.* 40 (S1), 124–138. doi:10.7623/syxb2019S1011

Liu, P., Jiang, Y. L., Liu, H., Wei, X., Li, K. C., and Zhu, R. W. (2013). The relationship between fault activity and hydrocarbon accumulation of Neogene in zhanhua depression, bohai bay basin. *Nat. Gas. Geosci.* 24 (3), 541–547. doi:10.11764/j.issn.1672-1926.2013.03.541

Liu, P., Zhang, X. T., Du, J. Y., Chen, W. T., Tao, W. F., and Tao, Y. (2018). Tectonic-thermal evolution process and its petroleum geological significance of relatively low geothermal gradient in rift basin: an example from Xi jiang main Sag in Pearl River Mouth Basin. *Geol. Sci. Technol. Inf.* 37 (2), 149–156. doi:10.19509/j.cnki.dzkq.2018.0221

Ma, B. S., Qi, J. F., Chen, W. C., and Zhao, M. (2018). Fault interaction and evolution during two-phase rifting in the Xijiang sag, Pearl River Mouth basin, northern south China sea. *Geol. J.* 55 (2), 1128–1147. doi:10.1002/gj.3474

Martínez Candela, A., Chiarella, D., Jackson, C. A.-L., Rennie, H., and Scarselli, N. (2024). Syn-rift tectono-stratigraphic development of the Thebe-0 fault system, Exmouth Plateau, offshore NW Australia: the role of fault-scarp degradation. *Basin Res.* 36 (1), 12842. doi:10.1111/bre.12842

Mi, L. J., Zhang, Z. T., Pang, X., Liu, J., Zhang, B., Zhao, Q., et al. (2018). Main controlling factors of hydrocarbon accumulation in Baiyun Sag at northern continental margin of South China Sea. *Earth Sci.* 45 (5), 963–973. doi:10.1016/s1876-3804(18)30100-9

Naseer, M. T. (2025). Quantitative appraisal of tectonically-influenced hydrocarbon-bearing Late-Cretaceous fluvial depositional system, Southwest Pakistan using spectral waveform-based instantaneous lateral thickness variability static simulations. *J. Asian Earth Sci.* 277, 106377. doi:10.1016/j.jseaes.2024.106377

Northrup, C. J., Royden, L. H., and Burchfiel, B. C. (1995). Motion of the Pacific plate relative to Eurasia and its potential relation to Cenozoic extension along the eastern margin of Eurasia. *Geology* 23 (8), 719–722. doi:10.1130/0091-7613(1995)023<0719:motppr>2.3.co;2

Pang, X., Zheng, J. Y., Ren, J. Y., Wang, F. G., Yan, H., Sun, H., et al. (2022). Structural evolution and magmatism of fault depression in Baiyun Sag, northern margin of South China Sea. *Earth Sci.* 47 (7), 2303–3231. doi:10.3799/dqkx.2022.064

Peters, K., Walters, C., and Moldowan, J. (2005). The Biomarker Guide. *Cambridge University Press* 1. doi:10.1017/CBO9780511524868

Qi, J. F., Yang, Q., Tong, H. M., and Lu, K. Z. (1997). Sequence construction response to tectonic process in extensional half-graben basin. *Earth Sci.* 22 (6), 603–608.

Reemst, P., and Cloetingh, S. (2000). Polyphase rift evolution of the Voring margin (mid Norway): constraints from forward tectonostratigraphic modeling. *Tectonics* 19 (2), 225–240. doi:10.1029/1999tc900025

Rosendahl, B. R., Reynolds, D. J., Lorber, P. M., Burgess, C. F., McGill, J., Scott, D., et al. (1986). *Structural expressions of rifting: lessons from lake tanganyika, africa*. London: Geological Society London, Special Publication 25, 29–43.

Ru, K. (1990). Half graben analysis of rift basin. *China Offshore Oil Gas* 4 (6), 1–10.

Schirripa, S. G., Bernasconi, S. M., Aldega, L., Castorina, F., Billi, A., Smeraglia, L., et al. (2024). Interplay and feedback between tectonic regime, faulting, sealing horizons, and fluid flow in a hydrocarbon-hosting extensional basin: the Val d'Agri Basin case, Southern Italy. *Earth Planet. Sci. Lett.* 646, 118982. doi:10.1016/j.epsl.2024.118982

Shi, H. S. (2013). On the uneven distribution of oil and gas resources and zoning difference enrichment: a sag of Pearl River Mouth Basin as an example. *China Offshore Hydrocarb.* 25 (5), 1–8.

Shi, H. S., Du, J. Y., Mie, L. F., Zhang, X. T., Hao, S. S., Liu, P., et al. (2020). Huizhou movement and its implications in Pearl River Mouth basin, China. *Petroleum Explor. Dev.* 47 (3), 1–12. doi:10.1016/S1876-3804(20)60067-2

Shi, H. S., Qin, C. G., Gao, P., Zhang, Z. T., Zhu, J. Z., and Zhao, R. Y. (2008). Late gas accumulation characteristics in Panyu low-uplift and the north slope of Baiyun sag, Pearl River Mouth Basin. *China Offshore Oil Gas.* 20, 73–76. (In Chinese with English Abstract).

Shi, H. S., Shu, Y., Du, J. Y., and Zhu, J. Z. (2017). *Paleogene petroleum geology in the eastern Pearl River Mouth basin*. Beijing: Geology Press.

Shi, H. S., Yu, S. M., Mei, L. F., Yu, Y., and Wu, J. Y. (2009). Features of Paleogene episodic rifting in Huizhou fault depression in the Pearl River Mouth basin. *Nat. Gas. Ind.* 29 (1), 35–37. doi:10.3787/j.issn.1000-0976.2009.01.008

Shi, S., Yang, W., Zhou, G., Jiang, H., Meng, H., Wu, S., et al. (2024). Impact of tethyan domain evolution on the formation of petroleum systems in the sichuan super basin, SW China. *Petroleum Exploration and Development* 51 (5), 1183–1198. doi:10.1016/S1876-3804(25)60534-9

Steckler, M. S. (1985). Uplift and extension at the Gulf of Suez: indications of induced mantle convection. *Nature* 317, 135–139. doi:10.1038/317135a0

Suo, Y. H., Li, S. Z., Dai, L. M., Liu, X., and Zhou, L. H. (2012). Cenozoic tectonic migration and basin evolution in East Asia and its continental margins. *Acta Petrol. Sin.* 28 (8), 2602–2618.

Tajmir, R. Z., Sarkarinejad, K., Faghih, A., Soleimany, B., and Payrovian, G. R. (2021). Impact of inversion tectonics on the spatial distribution of hydrocarbon traps in the NW Persian Gulf and the southern Dezful Embayment, SW Iran. *Mar. Petroleum Geol.* 134, 105364. doi:10.1016/j.marpetgeo.2021.105364

Tian, R., Xian, B., Liu, J., Wu, Q., Rahman, N. U., Chen, P., et al. (2024). Variability of sequence architecture in a rift margin controlled by tectonic activity: the Eocene Dongying Depression, Bohai Bay Basin, China. *Basin Res.* 36 (3), 12876. doi:10.1111/bre.12876

Wang, J. H., Pang, X., Wang, H., Liu, B. J., and Chen, X. X. (2024). Tide current-reworked sandy submarine fan deposits in Miocene zhujiang formation, Baiyun sag of Pearl River Mouth basin. *Earth Sci.* 49 (1), 71–83. doi:10.3799/dqkx.2022.334

Wang, L., Xie, X. L., Liu, S. X., Song, S., and Sun, R. (2017). Analysis of hydrocarbon accumulation and diversity of the major basins in mid-southern part of the South China Sea. *Nat. Gas. Geosci.* 28 (10), 1546–1554. doi:10.11764/j.issn.1672-1926.2017.08.010

Wang, W., Ye, J. R, Y, X. H., Shi, H. S., Shu, Y., and Wu, J. (2015). Sediment provenance and depositional response to multistage rifting, Paleogene, Huizhou depression, Pearl River Mouth basin. *Earth Sci.* 40 (6), 1061–1071. doi:10.3799/dqkx.2015.088

Wu, K. Q., Wu, J. F., Liu, L. F., Huang, S. B., and Li, C. R. (2014). Tectonic transport and its impact on hydrocarbon accumulation: two cases of Bodong and Miaoxi sag. *China Offshore Oil Gas* 26 (2), 6–11.

Xia, B., Lv, B. F., Wu, G. G., Cheng, G. W., Li, W. Q., and Wang, Y. (2007). The Cenozoic tectonic transport and its control on the source rock in the northern South China Sea. *Nat. Gas. Geosci.* 18 (5), 629–633. doi:10.3969/j.issn.1672-1926.2007.05.001

Xie, X. L., Cheng, S. T., and Lu, Y. C. (1996). Episodic tectonic cycles and internal architectures of sequences in continental basin. *Earth Sci.* 21 (1), 27–33.

Ye, Q., Shi, H. S., Mei, L. F., Shu, Y., Liu, H. L., Tian, W., et al. (2017). Post-Rift faulting migration, transition and dynamics in Zhu I depression, Pearl River Mouth basin. *Earth Sci.* 42 (1), 105–118. doi:10.3799/dqkx.2017.008

Yin, S., Ahmed, E., Radwan, A., Xiao, F., and Lai, P. (2024). Developmental characteristics of vertical natural fracture in low-permeability oil sandstones and its influence on hydraulic fracture propagation. *Geomech. Geophy Geo Energy Geo Res.* 10, 165. doi:10.1007/s40948-024-00889-0

Zeng, B., Qu, J., Mi, Z., Xie, E., Fu, H., Yang, S., et al. (2025). The control of effective source rocks on the distribution of hydrocarbon reservoirs in a lacustrine rift-basin: insights from a 3D basin modeling study. *Journal of Petroleum Exploration and Production Technology* 15 (1), 21. doi:10.1007/s13202-024-01888-3

Zhang, G. C., Li, Y. C., Xie, X. J., and Wang, Y. B. (2016). Tectonic cycle of marginal sea controls the ordered distribution of source rocks of deep water areas in South China Sea. *China Offshore Oil Gas* 28 (2), 23–26. doi:10.11935/j.issn.1673-1506.2016.02.003

Zhang, X. T., Wang, X. D., Shu, Y., Zhang, S. F., Que, X. M., Yu, Q. H., et al. (2017). Geological characteristics and forming conditions of large and medium oilfields in lufeng sag of eastern Pearl River Mouth basin. *J. Central South Univ. Sci. Technol.* 48 (11), 2979–2989. doi:10.11817/j.issn.1672-7207.2017.11.019

Zhao, Y. H. (2016). *Basin architecture and its evolution mechanism of Baiyun Sag, northern margin of the South China Sea*. Wuhan: China University of Geosciences. Doctoral dissertation.

Zhong, Z. H., Shi, H. S., Zhu, M., Pang, X., He, M., Zhao, Z. X., et al. (2014). A discussion on the tectonic-stratigraphic framework and its origin mechanism in Pearl River Basin. *China Offshore Oil Gas* 26, 20–29.

Zhou, Z., Peng, W., Sun, H., Feng, K., and Zhu, W. (2024). Coupling relationship between basin evolution and hydrocarbon reservoirs in the northern central myanmar basin: insights from basin and petroleum system modeling. *Journal of Marine Science and Engineering* 12 (9), 1497. doi:10.3390/jmse12091497

Zhu, H. T., Li, S., Liu, H. R., Shu, Y., Mei, L. F., and Yang, X. H. (2016). The types and implication of migrated sequence stratigraphic architecture in continental lacustrine rift basin: an example from the Paleogene Wenchang Formation of Zhu I Depression, Pearl River Mouth Basin. *Earth Sci.* 41 (3), 361–372. doi:10.3799/dqkx.2016.028

Zhu, J. Z., Shi, H. S., Long, Z. L., Du, J. Y., Shu, Y., and Shi, Y. (2015). Accumulation pattern and hydrocarbon distribution of half-graben accumulation system in Zhuyi Depression. *China Pet. Explor.* 20 (1), 24–36. doi:10.3969/j.issn.1672-7703.2015.01.003

Zhu, P. (2007). Petroleum system analysis of the northern sag, the southern yellow sea basin. *Petroleum Geol. Exp.* 29 (6), 549–553. doi:10.11781/sysydz549

Zhu, Y. H., Zhu, W. L., Xu, Q., Wang, Y. M., and Lu, M. (2009). Sedimentary characteristics and sequence framework of the zhuhai-zhujiang Formation in the middle area of Pearl River Mouth basin. *Mar. Geol. Quat. Geol.* 29, 77–80. doi:10.3724/SP.J.1140.2009.04077

Zhuo, H., Wang, Y., Shi, H., He, M., Chen, W., Li, H., et al. (2015). Contrasting fluvial styles across the mid-Pleistocene climate transition in the northern shelf of the South China Sea: evidence from 3D seismic data. *Quatern. Sci. Rev.* 129, 128–146. doi:10.1016/j.quascirev.2015.10.012